AFRL-AFOSR-VA-TR-2020-0160

Hot-Electrons Generation in New Plasmonic Materials for Integrated On-Chip Devices

Alexandra Boltasseva
PURDUE UNIVERSITY

07/25/2020
Final Report

Air Force Research Laboratory
AF Office Of Scientific Research (AFOSR)/ RTB1
Arlington, Virginia 22203
Air Force Materiel Command

DISTRIBUTION A: Distribution approved for public release.

REPORT DOCUMENTATION PAGE

Form Approved
OMB No. 0704-0188

1. REPORT DATE *(DD-MM-YYYY)*	2. REPORT TYPE	3. DATES COVERED *(From - To)*
01-09-2020	Final Performance	27 Apr 2017 to 26 Apr 2020

4. TITLE AND SUBTITLE
Hot-Electrons Generation in New Plasmonic Materials for Integrated On-Chip Devices

5a. CONTRACT NUMBER

5b. GRANT NUMBER
FA9550-17-1-0243

5c. PROGRAM ELEMENT NUMBER
61102F

6. AUTHOR(S)
Alexandra Boltasseva, Vladimir Shalaev

5d. PROJECT NUMBER

5e. TASK NUMBER

5f. WORK UNIT NUMBER

7. PERFORMING ORGANIZATION NAME(S) AND ADDRESS(ES)
PURDUE UNIVERSITY
401 SOUTH GRANT ST
WEST LAFAYETTE, IN 47907-2024 US

8. PERFORMING ORGANIZATION REPORT NUMBER

9. SPONSORING/MONITORING AGENCY NAME(S) AND ADDRESS(ES)
AF Office of Scientific Research
875 N. Randolph St. Room 3112
Arlington, VA 22203

10. SPONSOR/MONITOR'S ACRONYM(S)
AFRL/AFOSR RTB1

11. SPONSOR/MONITOR'S REPORT NUMBER(S)
AFRL-AFOSR-VA-TR-2020-0160

12. DISTRIBUTION/AVAILABILITY STATEMENT
A DISTRIBUTION UNLIMITED: PB Public Release

13. SUPPLEMENTARY NOTES

14. ABSTRACT
In this project, in collaboration with ETH, Zurich, a record-breaking, ultra-compact, low-loss plasmonic modulator with 72Gbps speed and a power consumption of 12 fJ/bit was demonstrated (year 1). In year 2, we demonstrated hybrid plasmonic waveguides utilizing ultrathin TiN films that outperform gold waveguides in terms of mode compactness and propagation length. We also performed systematic studies of TiN, ZrN, ZnO, TiO films and nanoparticles that laid the foundation for the subsequent work. A comprehensive review of plasmonics for energy harvesting was carried out, and efficient water-splitting application assisted by gap-plasmons was demonstrated. In year 3, we explored plasmonics for color generation and demonstrated plasmonic color printing with semicontinuous metal films. We showed that TiN@Ti02 core-shell nanoparticles act as plasmon-enhanced photosensitizers. In addition to metals and semi metals, we investigated metal oxides and showed extraordinarily large permittivity and reflectance modulation in ZnO films and nanostructures. With broadband pump-probe spectroscopy, we measured the hot-carrier relaxation time in plasmonic TiN and ZrN films. In a collaborative effort, an advanced technique for the hot-carrier distribution mapping in plasmonic structures was invented. In the area of metasurfaces, we employed machine-learning-assisted computational methods to optimize the performance of high efficiency thermal emitters. Another collaborative effort lead to the demonstration of high-temperature-tolerant nanofurnaces with refractory TiN for heterogeneous catalysis. We also investigated the plasmonic properties of strongly correlated materials such as strontium niobite. A high-temperature sensor utilizing refractory plasmonic materials was shown as well. Finally, we quantified the spatial and temporal nanoscale plasmonic heating by thermoreflectance measuremen

15. SUBJECT TERMS
plasmonic materials, Hot-Electron Generation, Plasmonics, Integrated photonics, Nanophotonics, Nanoelectronics, Surface plasmons

16. SECURITY CLASSIFICATION OF:			17. LIMITATION OF ABSTRACT	18. NUMBER OF PAGES	19a. NAME OF RESPONSIBLE PERSON
a. REPORT	b. ABSTRACT	c. THIS PAGE			POMRENKE, GERNOT
Unclassified	Unclassified	Unclassified	UU		19b. TELEPHONE NUMBER *(Include area code)* 703-696-8426

Final Report: 07/26/2020

Hot-Electron Generation in New Plasmonic Materials for Integrated On-Chip Devices

AFOSR Grant # FA9550-17-1-0243

PI: Prof. Alexandra Boltasseva, Purdue University

PM: Dr. Gernot Pomrenke

1. Summary

Plasmonics, or metal-based nano-optics, promises to bring significant advances to the generation, processing, transmission, and detection of signals at optical frequencies and at the ultra-compact scales for applications in the fields of optical communications [1], sensing [2], energy conversion and photocatalysis [3]. The current project focuses on both gaining fundamental insights into the dynamics of hot-carrier physics in plasmonic devices as well as on experimental demonstration of practical plasmonic devices. With industry-relevant materials such as transparent conducting oxides and transition metal nitrides, we developed tailorable, electrically and optically tunable devices for the emerging field of hybrid electronic/photonic circuitry. Specifically, we demonstrated long-range plasmonic waveguides utilizing titanium nitride as plasmonic material that outperformed gold in its optical performance. We also explored the area of plasmonics for energy; and employed machine learning algorithms to optimize broadband plasmonic metasurfaces that act as high efficiency thermal emitters. Furthermore, we performed dynamic optical characterizations on zinc oxide to demonstrate extraordinary permittivity and reflectance modulation. The results and findings of this project contribute to deeper understanding of hot-carrier dynamics in metals and oxides, and aid in the development of the next generation of spatial light modulators, more efficient and secure optical, optoelectronic and quantum systems as well as photocatalytic applications.

This report presents a summary of the results accomplished over the duration of the project. Sections 2.1 and 2.2 summarizes the publications reported in previous years. Section 2.3 summarizes the ongoing and completed works accomplished in the final year of the project.

In year 1, in collaboration with ETH, Zurich, a record-breaking, ultra-compact, low-loss plasmonic modulator with 72Gbps speed and a power consumption of 12 fJ/bit was demonstrated. We also developed an advanced experimental setup to map the hot-carriers distribution in plasmonic nanostructures. In year 2, we demonstrated hybrid plasmonic waveguides utilizing ultrathin TiN films that outperform noble metal waveguides in terms of mode compactness and propagation length. We also performed material characterizations of TiN, ZrN and ZnO films, and TiN and TiO2 nanoparticles that laid the foundation for the subsequent work. A comprehensive review of plasmonics for energy harvesting was carried out, and efficient water-splitting application assisted by gap-plasmons was demonstrated. In year 3, we explored plasmonics for color generation and demonstrated plasmonic color printing with semicontinuous metal films. We showed that TiN@TiO_2 core-shell nanoparticles act as plasmon-enhanced photosensitizers. In addition to metals and semimetals, we investigated metal oxides and showed extraordinarily large permittivity and reflectance modulation in ZnO films and nanostructures. With broadband pump-probe spectroscopy, we measured the hot-carrier relaxation time in plasmonic TiN and ZrN films. In a collaborative effort, an advanced technique to map the hot-carrier distribution in plasmonic structures was invented. In the area of plasmonic metasurfaces, we employed machine-learning-assisted computational methods to optimize the performance of high efficiency thermal emitters. Another collaborative effort lead to the demonstration of high-temperature-tolerant nanofurnaces with refractory TiN for heterogeneous catalysis. We also investigated the plasmonic properties of strongly correlated materials such as strontium niobite. A high-temperature sensor utilizing refractory plasmonic materials was shown as well. Finally, we quantified the spatial and temporal nanoscale plasmonic heating by thermoreflectance measurements.

The results of the project would enable a broader understanding of the conventional and emerging plasmonic materials and the temporal and spatial dynamics of plasmon-induced hot carriers for a wide range of applications.

2.1 Project Period: Apr 27, 2017 – Apr 26, 2018

A Low-Loss Plasmonic Modulator (Published in Nature)

The high field-confinement and sub-wavelength confinement of plasmonic structures make them suitable for the miniaturization of photonic components[4]. The large ohmic losses of plasmonics provides a challenge in the field. In collaboration with our partners in ETH Zurich, Switzerland, Virginia Commonwealth University, and University of Washington, we took part in the design of a low-loss, plasmon-assisted electro optic modulator. In this technique, light passes through a photonic waveguide in the 'on state', and is coupled to the lossy surface plasmon polaritons only in the device's 'off state' in which attenuation is desired.

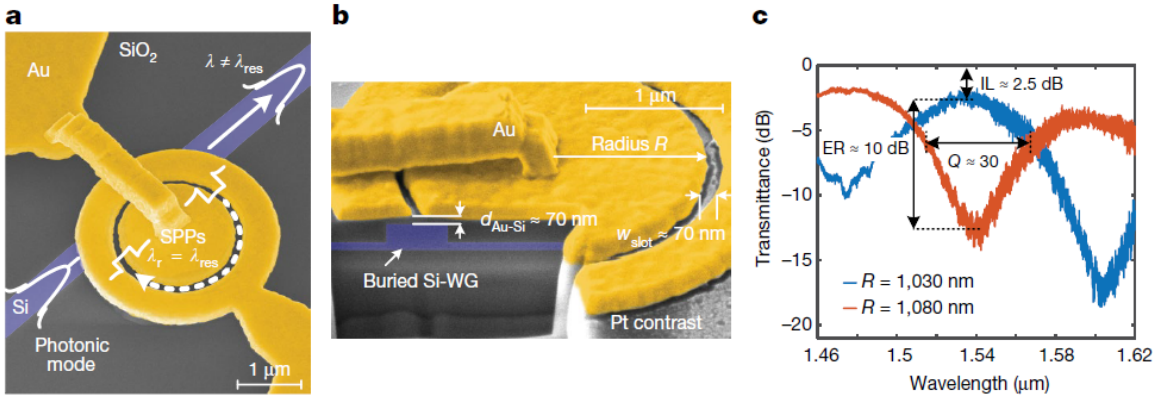

Figure 1. False-coloured scanning electron microscopy (SEM) image of a plasmonic ring resonator and the corresponding transmittance. a, Top view; b, cross-section of the resonator. Photonic modes propagating in the buried silicon waveguide (Si-WG) resonator couple partially to the SPPs in the MIM ring when the resonance condition is fulfilled. While out of resonance, operation results in low-loss light transmission. c, Passive measurements of two identical ring resonators that differ only in radii (blue, 1,030 nm; red, 1,080 nm).

The blue SOI waveguide passes the signal in the 'on' state (Fig 1(a)). A plasmonic slot-waveguide based ring resonator lies on top of the waveguide, with an oxide layer in the middle. An organic, electro optic polymer (OEO) fills the cavity in the slot. In the 'off-state', the refractive index of the polymer changes under an applied voltage using the suspended gold-bridge contacts. The propagating mode now couples into the resonator, killing the wave. The losses in a resonator type configuration can be reduced by more than 6 dB compared to MZI type configurations. In total, the ring device offers an advantage of 6 dB insertion loss over the MZI modulator because of its compactness and the bypass mechanism in the on-state. Losses can be further reduced by under-coupling the resonator, as limited extinction ratios of 10 dB are sufficient for many practical applications. The fabricated device operated at a 72Gbps with a bit-error-ratio of 1 x 10-3 in the off-resonant state, with an estimated power consumption of 12 $fJbit^{-1}$.

We have an ongoing project involving a similar resonator with TiN, which is on-hold because of equipment down-time and the lab-shutdowns because of COVID-19.

2.2 Project Period: Apr 27, 2018 – Apr 26, 2019

Hybrid Long-Range Plasmonic Interconnects (Published in ACS Photonics)

Long range surface plasmon polariton (LRSPP) waveguides comprise an insulator-metal-insulator geometry and have been utilized in integrated optical components [5], and sensing platforms[6] Conventional LRSPP design involves refractive index matching of the substrate and the superstrate, or complex, multilayer fabrication techniques. We demonstrate a hybrid photonic-plasmonic waveguide employing dielectric layers with a significant index mismatch. The waveguide achieves compact mode sizes and long-range propagation, outperforming conventional LRSPP waveguides.

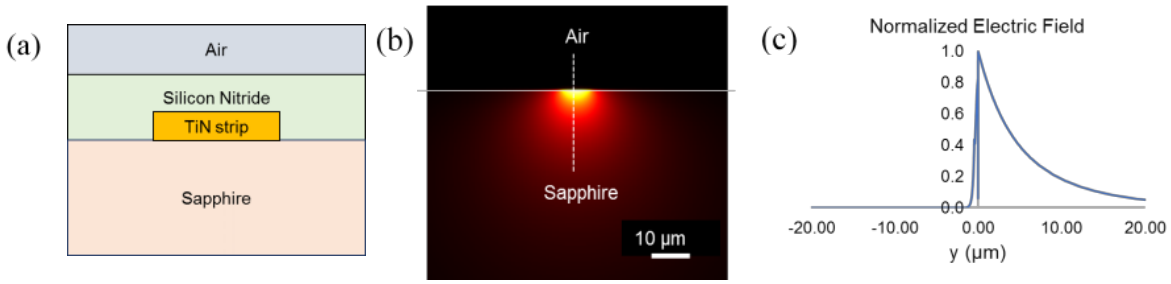

Figure 2. (a) Schematic of the hybrid photonic-plasmonic waveguide. (b) Mode-profile of the waveguide showing the normalized electric field across a vertical cross section. (c) Simulated modal profile showing the normalized electric field |E|, from the FEM Multiphysics. (d) Experimentally obtained mode-profile of the fabricated TiN waveguide. (e) Mode size, propagation length, and FOMs of TiN HPP waveguides with different cladding materials on sapphire.

The structure is a 8.8-nm high, 8.7-µm wide strip of TiN on a sapphire substrate with a silicon nitride cladding (Fig 2(a). 2(b) illustrates the normalized mode profile simulated with the finite element method (FEM) in the frequency domain. Fig. 2c shows the field distribution in the waveguide. The guided wave has an asymmetric, sinusoidal electric field distribution in the superstrate, and an exponential decay in the substrate, highlighting the hybrid nature of the mode. The average mode size of the fabricated device was found to be 7.7 µm, closely matching simulations (7.75 µm). The propagation length, measured by cut-back method was 7.2 mm (7.5 mm in simulations). The fabricated waveguide has a figure of merit of 534 (defined as the ratio of the propagation length to the normalized mode size and the effective mode index), surpassing the values reported previously for long-range, surface plasmon polariton waveguides made of gold (FOM = 229) [5]and TiN (FOM = 321) [7]. This design enables the matching of substrates and superstrates based on different applications, like photonic circuits, loss compensation, or optical modulation.

Plasmonics for Energy Storage (Review published in Advanced materials) and gap-plasmon induced water splitting (Published in Faraday Discussions)

Iron oxide (a-Fe2O3), or hematite, is one of the more promising candidate materials for solar water splitting, with a theoretical STH efficiency of 15%. In this work, experimentally increase water oxidation photocurrent by utilizing gold nanostructures that support gap-plasmon resonances together with a hematite layer. The increase is two times over that demonstrated by a bare hematite film at wavelengths above the hematite bandgap. Moreover, we achieve a six-fold increase in the oxidation photocurrent at near-infrared wavelengths, via hot electron generation and decay in the gap-plasmon nanostructures. Fig. 3 summarizes the findings in this project.

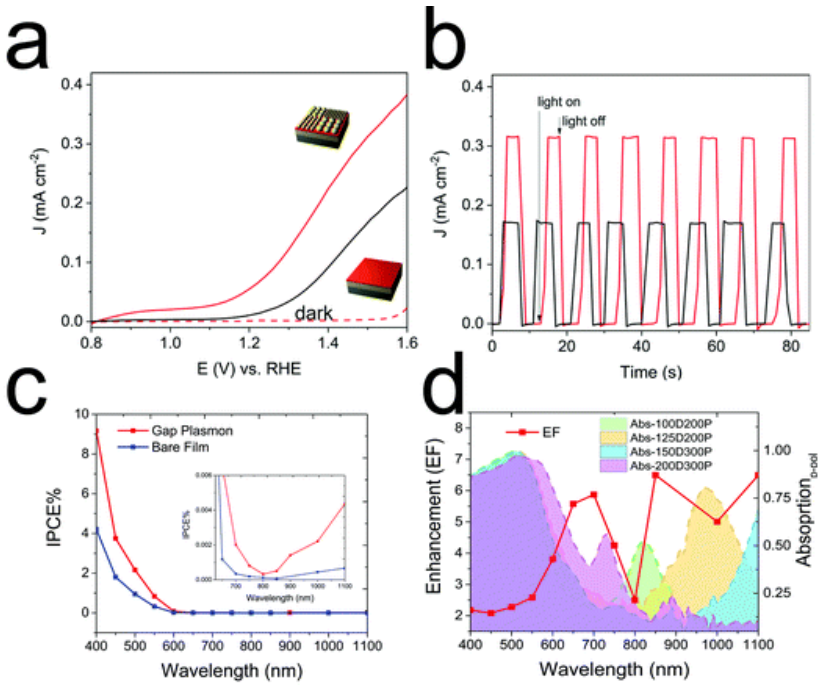

Figure 3. (a) Linear sweep voltammetry measurements with a 3 electrode PEC cell for gold-hematite gap-plasmon and bare hematite films. (b) Chopped photocurrent measured at 1.5 V vs. RHE for the two samples. The photocurrent from the gap-plasmon resonators is almost 2 times that of the bare flat hematite electrode. (c) Incident Photon Conversion Efficiency (IPCE) for the gap-plasmon electrode and bare hematite electrode at 1.5 V of applied bias vs. RHE. (d) Enhancement Factor (EF) of the IPCE for the gap-plasmon electrode with all four nanostructure arrays and a bare film. Above the hematite bandgap, the gap-plasmon electrode exhibits approximately twice the efficiency of the bare electrode. Below the bandgap, the increase in efficiency is up to six/seven-fold.

2.3 Project Period: Apr 27, 2019 – July 26, 2020

Review of Plasmonics for Color Applications (Published in Applied Physics Reviews) and Plasmonic Color Printing with Semicontinuous Metal Films (published in OMEx)

We performed an extensive review of the application of plasmonics in color applications. We extended the works by demonstrating plasmonic color printing with semicontinuous metal films. Plasmonic color printing with semicontinuous metal films is a lithography-free, non-fading, and environmentally friendly method of generation of bright colors[8]. Their color filtering effects are a consequence of the resonant coupling of light and free electrons in metal nanoparticles, known as surface plasmons, that confine light at the nanoscale and lead to the enhancement of the local electromagnetic field. Semicontinuous metal films (SMF), which are randomly distributed metal nanoparticles at the near-percolation regime, can offer both plasmonic sub-wavelength color resolution and large-scale, low-cost fabrication. Random, fractal-type island SMFs are comprised of nanoparticles of diverse sizes and shapes resonating at different wavelengths. When illuminated with high-intensity laser light, thermal effects modify nanoparticles in SMFs, leading to variations in the optical response, and hence, generation of different colors. We have demonstrated a wide range of plasmonic colors generated by a silver SMF on a silver mirror with a dielectric spacer (SMF/M). This structure utilizes the so-called gap-plasmon modes and generates colors in the reflection mode. An ultrafast Ti: Sapphire femtosecond laser (1 kHz, 80 fs, 800 nm, linear polarization) is used to structurally modify the Ag nanoparticles for respective color generation through varying the laser parameters. We obtain intricate artistic designs with the in-house built laser scanning setup. In addition to color printing and arts, the demonstrated sub-micrometer resolution technique could pave the way to security and optical data storage applications while successfully addressing the challenges of scalability and toxicity across multiple technologies. Figure 4 comprises an overview of the results.

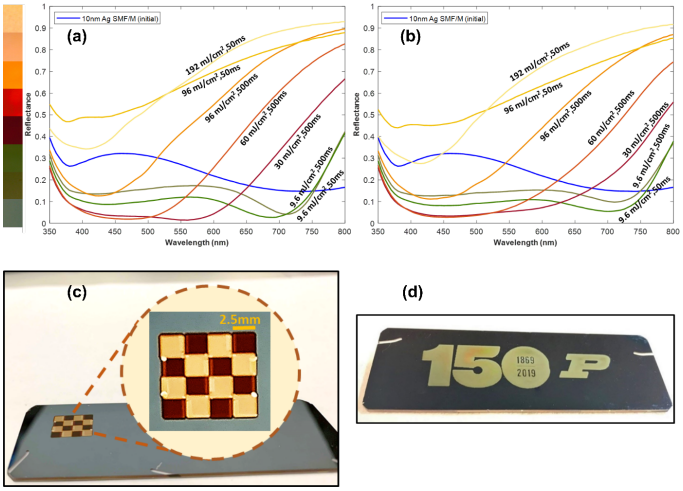

Figure 4. Reflectance spectra of overcoated 10 nm Ag SMF/M structure photomodified with different laser fluence measured with linearly polarized light (a) co-polarized and (b) cross-polarized with respect to laser polarization. The inset squares represent the generated color palette recorded using unpolarized light. Optical images of laser printed (a) checkered pattern (red - 30 mJ cm-2; yellow - 150 mJ cm-2) and (b) 150 years of Purdue logo with a "P" letter (100 mJ cm-2) on the SMF/M film.

TiN@TiO_2 Core-Shell Nanoparticles as Plasmon-Enhanced Photosensitizers: The Role of Hot-Electron Injection (Published in LPR)

Metal–semiconductor heterostructures have attracted a lot of attention due to their ability to enhance photovoltaic and photocatalytic processes[9]. Thus far, most of the proposed heterostructures are designed with noble metals, and the potential of alternative plasmonic materials, such as titanium nitride (TiN), is not yet well explored. In this work, TiN@TiO2 core-shell nanoparticles (NPs) are synthesized and proposed as plasmon-enhanced photosensitizers for efficient singlet oxygen generation, with the focus on the role of hot electron injection. Excitation of TiN@TiO2 NP dispersions by a 700 nm femtosecond-pulsed laser effectively converts ground-state oxygen into singlet oxygen (1O2), driven primarily by hot electrons generated during plasmon decay at the TiN–TiO2 interface and injected into the TiO2 layer. Considering the chemical inertness and low cost of TiN, TiN@TiO2 NPs hold great potential as plasmonic photosensitizers for photodynamic therapy and other photocatalytic applications at red-to-near-infrared wavelengths. Fig. 5 illustrates a schematic of the mechanism.

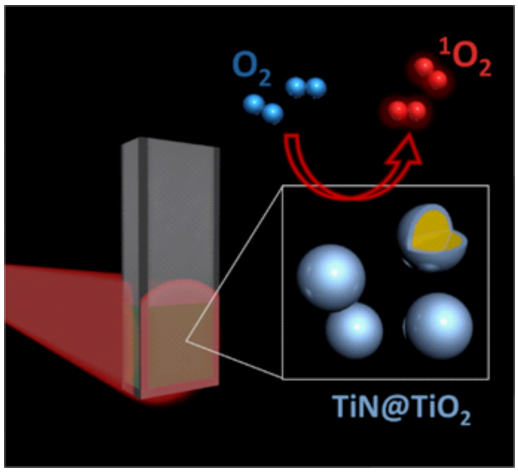

Figure 5. Illustration of the photocatalysis experiment. A laser illuminating a cuvette containing the nanoparticles supplies the energy for the catalytic breakdown of water, releasing free-radicals

Extraordinarily Large Permittivity Modulation in Zinc Oxide for Ultrafast Active Nanophotonics (Manuscript in Progress)

The dielectric permittivity of a material encapsulates the essential physics of light-matter interaction into the material's local response to optical excitation. Dynamic, photo-induced modulation of the permittivity can enable an unprecedented level of control over the phase, amplitude, and polarization of light[10]. Therefore, the detailed dynamic characterization of technology-relevant materials with substantially tunable optical properties and fast response times is a crucial step in the realization of tunable optical devices. This work reports on the extraordinarily large permittivity changes in zinc oxide thin films (up to -3.6 relative change in the real part of the dielectric permittivity at 1600 nm wavelength), induced by optically generated free carriers. We demonstrate broadband reflectance modulation up to 70% in metal-backed oxide mirrors at the telecommunication wavelengths, with picosecond-scale relaxation times. We show that the modulation can be selectively enhanced at specific wavelengths employing a hybrid plasmonic resonator while maintaining picosecond-scale switching times (Fig. 6). This work provides insights into the free-carrier assisted permittivity modulation in zinc oxide and could enable novel active devices for beam-steering, polarizers, and spatial light modulators.

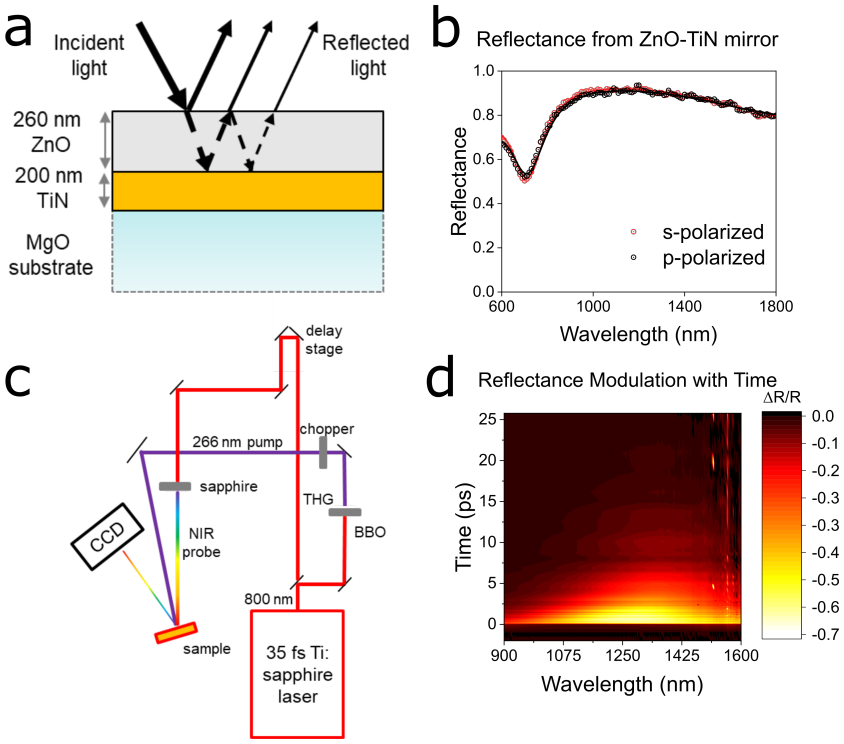

Figure 6. (a) Schematic of the TiN-ZnO mirror. The incident probe light makes multiple passes in the dielectric ZnO as it is reflected by the TiN-ZnO and ZnO-air interfaces. (b) Steady-state reflectance of s and p polarized light measured at 20° angle of incidence. The dots represent the measured reflectance and the solid lines represent the simulated reflectance computed using the optical properties of the layers via the transfer matrix method. (c) Pump-probe setup. (d) Color map showing the temporal (vertical-axis) and spectral (horizontal axis) dynamics of the reflection modulation under an interband pump at a pump fluence of 31.6 mJ/cm^2. The maximum modulation is around -70%, the negative sign corresponding to a decrease in the reflectance in the pumped state.

Investigation of Carrier Dynamics in Refractory metals (Published in OMEx) and Broadband Ultrafast Dynamics of Refractory Metals: TiN and ZrN (Published in AOM, in press)

Transition metal nitrides have recently gained attention in the fields of plasmonics, photocatalysis, photothermal applications, and nonlinear optics because of their optical properties, refractory nature, and large laser damage thresholds. This work reports comparative studies of the transient response of films of titanium nitride, zirconium nitride, and Au under femtosecond excitation. Broadband transient optical characterization helps to adjudicate earlier inconsistent reports regarding hot-electron lifetimes based upon single wavelength measurements. These pump-probe experiments show sub-picosecond transient dynamics only within the epsilon-near-zero window of the refractory metals. The dynamics are dominated by photoinduced interband transitions resulting from ultrafast electron energy redistribution. The enhanced reflection modulation in the epsilon-near-zero window makes it possible to observe the ultrafast optical response of these films at low pump fluences. These results indicate that electron-phonon coupling in TiN and ZrN is 25-100 times greater than in Au. Strong electron-phonon coupling drives the sub-picosecond optical response and facilitates greater lattice heating compared to Au, making TiN and ZrN promising for photothermal applications. The 2 spectral response and dynamics of TiN and ZrN are only weakly sensitive to pump fluence and pump excitation energy. However, the magnitude of the response is much greater at higher pump photon energies and higher fluences, reaching peak observed values of 15 % in TiN and 50 % in ZrN in the epsilon-near-zero window.

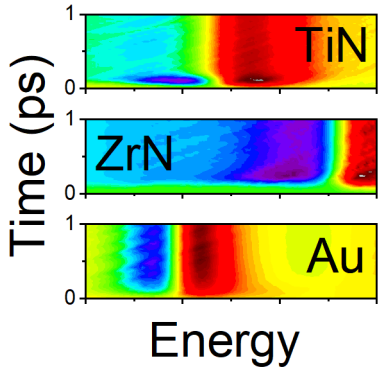

Figure 7. Spatiotemporal color map showing the relaxation dynamics of hot carriers in TiN, ZrN and Au versus time.

Revealing the energy spectrum of plasmonic hot-carriers (Published in Science)

The generation of hot-carriers in plasmonic nanostructures, via plasmon decay, is of great current interest as hot-carriers play key roles in applications like photocatalysis, energy harvesting, and in novel photodetection schemes that circumvent band-gap limitations. However, experimental quantification of steady-state energy distributions of hot-carriers in plasmonic nanostructures, which is critical for systematic progress, has not been possible. We recently developed an experimental approach that has enabled the direct measurement of hot-carrier energy distributions under steady-state conditions. Specifically, we showed how a scanning probe-based technique that records charge transport through single molecular junctions, when combined with nanoplasmonic experimental methods, can be leveraged to directly quantify hot-carrier energy distributions in a key model system—a thin gold film that supports propagating surface plasmon polaritons. Furthermore, using the above-outlined technique, we obtained key physical insights from our measurements on the role of Landau damping in producing hot-carriers and the contributions of different plasmonic modes towards hot-carrier generation.

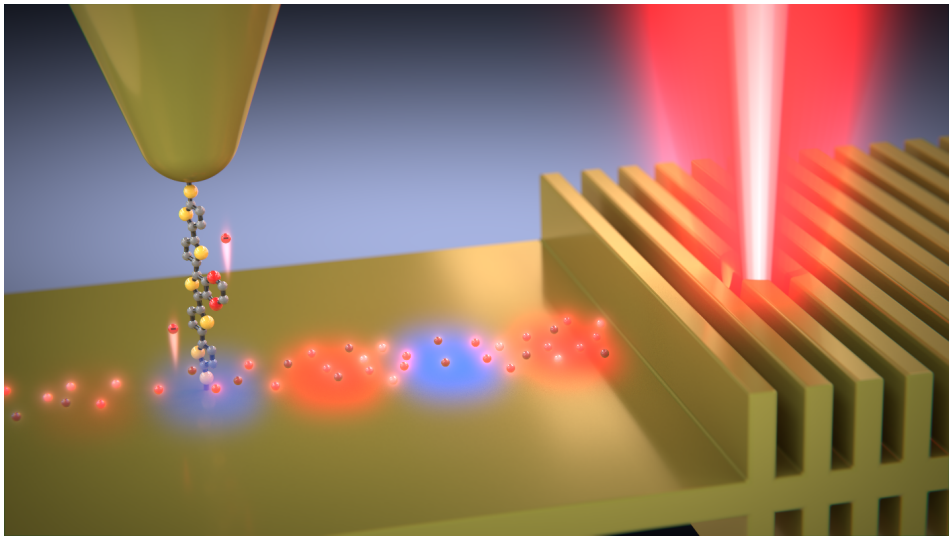

Figure 8. Graphic representation of the experimental approach to determine the energy distributions of plasmonic hot-carriers in a thin gold film. Surface plasmon polaritons are excited by illuminating the grating coupler with a laser, which leads to the generation of hot-carriers. The energy distributions of the generated hot-carriers are measured from the current flowing through a (voltage controlled) tunable molecular filter that selectively allows transport of carriers in a narrow energy window.

Machine-learning-assisted metasurface design for high-efficiency thermal emitter optimization (Published in Applied Physics Reviews)

Nanophotonic devices can provide solutions to challenges in energy conversion, information technologies, chemical or biological sensing, quantum computing, and secure communications. The realization of practical optical structures and devices is a complex problem due to the multitude of constraints on their optical performance, materials, scalability, and experimental tolerances, all of which are requirements implying large optimization spaces. However, despite the complexity of the process, to date, almost all nanophotonic structures are designed either intuitively or based on *a priori* selected topologies, and by adjusting a limited number of parameters. These intuition-based models are limited to *ad hoc* needs and have narrow applicability and predictive power, with the exhaustive parameter searches often performed manually. Since the comprehensive search in hyper-dimensional design space is highly resource-heavy, multi-objective optimization has so far been almost impossible. Humans' restrained capacity to think hyper-dimensionally also limits the perception of multivariate optimization models, and, therefore, advanced machinery is needed to manage the multi-domain, hyper-dimensional design parameter space. In this work, we merge the topology optimization method with deep learning algorithms, such as adversarial autoencoders, and show substantial improvement of the optimization process in terms of computational time (4900 times faster) and final devices efficiencies (~98%) by providing unparalleled control of the compact design space representations (Fig. 9). By enabling efficient, global optimization searches within complex landscapes, the proposed compact hyperparametric representations could become crucial for multi-constrained problems. The proposed approach could enable a much broader scope of the optimal designs and data-driven materials synthesis that goes beyond photonic and optoelectronic applications.

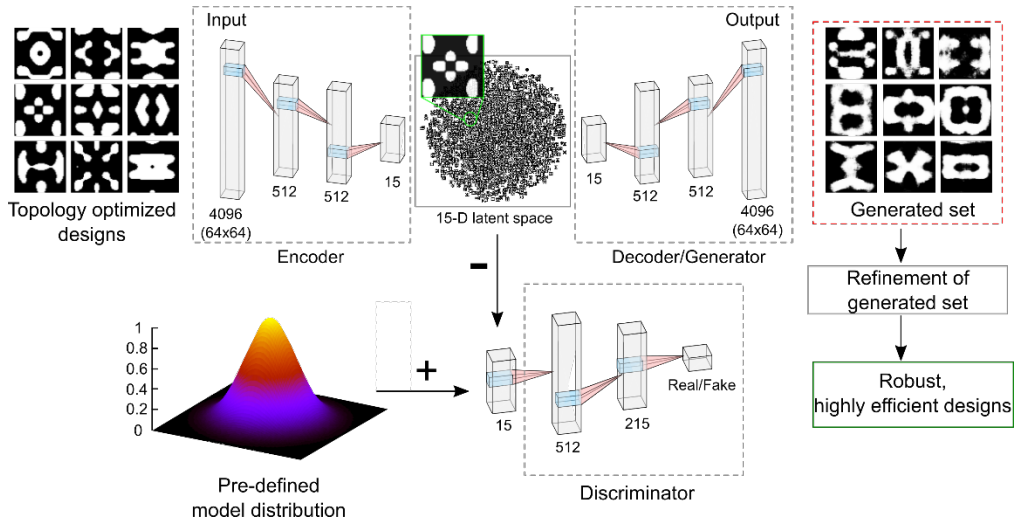

Figure 9. Schematic for machine learning assisted photonic design.

Solar Thermoplasmonic Nanofurnace for High-Temperature Heterogeneous Catalysis (Published in Nano Letters)

Most existing solar thermal technologies require highly concentrated solar power to operate in the temperature range 300−600 °C. Here, thin films of refractory plasmonic TiN cylindrical nanocavities manufactured via a flexible and scalable process are presented. The fabricated TiN films show polarization-insensitive 95% broadband absorption in the visible and near-infrared spectral ranges and act as plasmonic "nanofurnaces" capable of reaching temperatures above 600 °C under moderately concentrated solar irradiation (~20 Suns). The demonstrated structures can be used to control nanometer-scale chemistry with zeptoliter (10−21 L) volumetric precision, catalyzing C-C bond formation and melting inorganic deposits. Also shown is the possibility to perform solar thermal CO oxidation at rates of 16 mol h^{-1} m^{-2} and with a solar-to-heat thermoplasmonic efficiency of 63%. Access to scalable, cost-effective refractory plasmonic nanofurnaces opens the way to the development of modular solar thermal devices for sustainable catalytic processes.

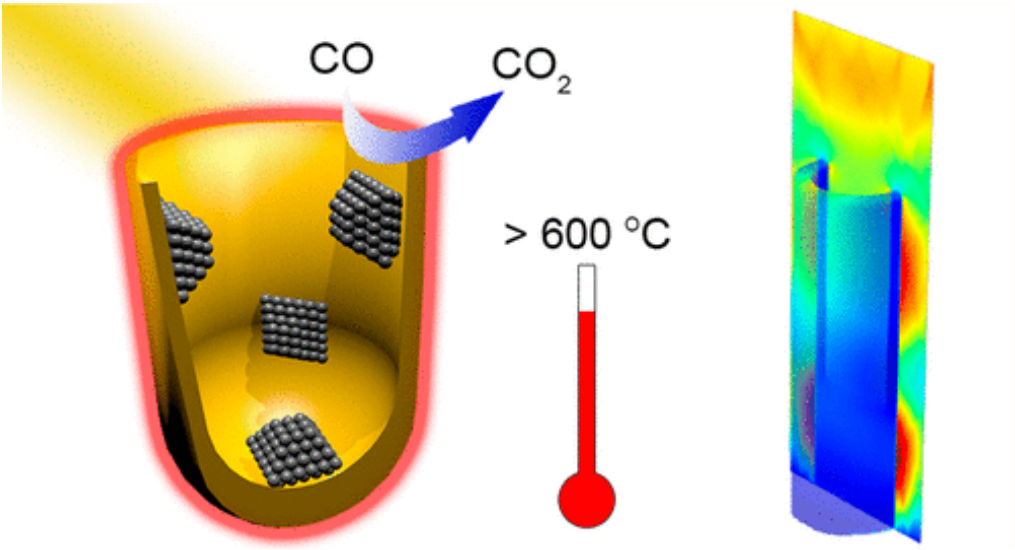

Figure 10. Illustration of heterogeneous catalysis at high temperature.

Strontium Niobate for Near-Infrared Plasmonics (Published in Advanced Optical Materials)

Plasmonics has developed greatly over the past two decades, and a plethora of plasmonic materials has been explored for practical plasmonic devices. While noble metals such as gold and silver are the most widely used plasmonic materials, other metals such as aluminum, copper, and magnesium have also been proposed as building blocks for plasmonics. Transparent conducting oxides (TCOs). These materials have lower carrier concentration than noble metals and therefore have lower material losses at the NIR. In this paper, strontium niobate (SNO) is showcased as an addition to the material database for plasmonics in the NIR. SNO plasmonic properties are studied through experimental demonstration of hybrid plasmon resonances in SNO films. Such resonances are characterized by electromagnetic field concentration in a low-index dielectric, sandwiched between a high-index dielectric resonator and a plasmonic metal. Although SNO bulk film has an order of magnitude greater carrier concentration than TCOs, its losses are only a few times higher than in TCO materials thus holding a promise for plasmonic applications in the NIR. Fig. 11 summarizes the findings.

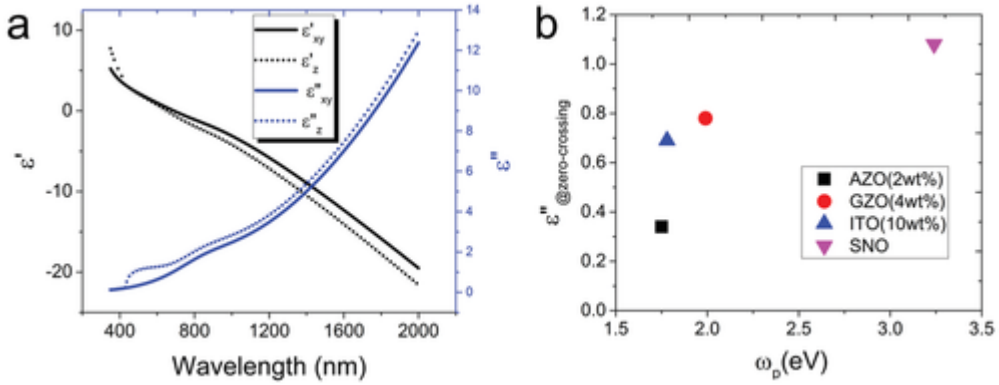

Figure 11. (a) Optical constants of 200 nm SNO on LSAT extracted from spectroscopic ellipsometry. The film shows uniaxial anisotropy. (b) Comparison of the imaginary part of permittivity at the zero-crossover wavelength of the real part of permittivity for SNO and other TCOs.

Remote Sensing of High Temperatures with Refractory, Direct-Contact Optical Metacavity (Published in ACS Photonics)

We utilized the temperature-dependent optical properties of refractory plasmonic transition metal nitrides and dielectric thin films to realize a planar, direct-contact, nanophotonic metacavity for remote, all-optical sensing of a wide range of surface temperatures (from room temperature to above 1000 °C). The hybrid metacavity device integrates the plasmonic cavity with a planar metasurface (Fig. 12) that utilizes refractory material components, namely, titanium nitride (TiN) and silicon nitride (Si3N4), and operates in a spectral wavelength window of 900–1400 nm. The thermally variant optical properties of the constituent materials (TiN, Si3N4) enable metacavity operation with a strong polarization-dependent resonant reflectance response. At the cavity resonance, relative amplitude variations of above 30% are detected in the temperature-dependent reflectance spectra that act as the read-out from the experimentally demonstrated sensor. The proposed high-efficiency, planar optical refractory sensor located directly on hot surfaces also allows for great scalability. The device enables true remote all-optical measurements by keeping other ancillary systems outside of the hot ambient conditions and, therefore, is especially relevant for applications in harsh environments.

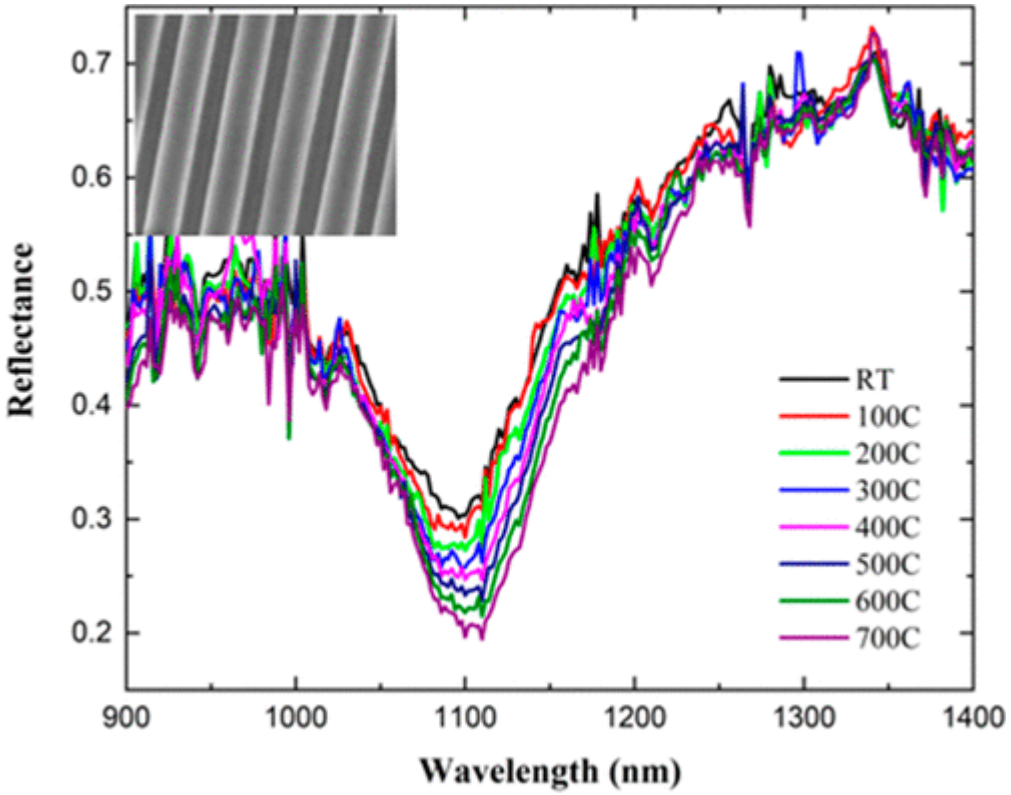

Figure 12. Experimental reflectance spectra of the metasurface (shown in the inset) at different temperatures.

Spatial and Temporal Nanoscale Plasmonic Heating Quantified by Thermoreflectance (published in Nano Letters)

Thermoplasmonics has thrived in the past decades because it uniquely provides remotely controllable nanometer-scale heat sources that have augmented numerous technologies. The dynamic behavior of the plasmonic heaters in the nanosecond regime has remained largely unexplored, yet such a time scale is indeed essential for a broad range of applications such as photocatalysis, optical modulators, and detectors. Here, we use two distinct techniques based on the temperature-dependent surface reflectivity of materials, optical thermoreflectance imaging (OTI) and time-domain thermoreflectance (TDTR), to comprehensively investigate plasmonic heating in both spatial and temporal domains. OTI enables the rapid visualization of plasmonic heating with sub-micron resolution outperforming a standard thermal camera, allowing us to establish the connection between the optical absorptance and heating efficiency and to analyze plasmonic heating dynamics on the millisecond scale. The TDTR technique allows us to study the optical resonance-dependent heat-transfer dynamics of a nanometer-scale plasmonic structure in the nanosecond regime and use a detailed computational model to extract the impulse response and thermal interface conductance of a multilayer plasmonic structure (Fig. 13). The study reveals a quantitative relationship between the dimensions of the nanopatterned structure and its spatiotemporal thermal response to the light pulse excitation, a thermoplasmonic effect resulting from the spatial distribution of the absorbed electromagnetic energy. We also conclude that the two thermoreflectance techniques provide necessary feedback to nanoscale thermoplasmonic heat management, for which optimization in either heating power or temperature decay speed is needed.

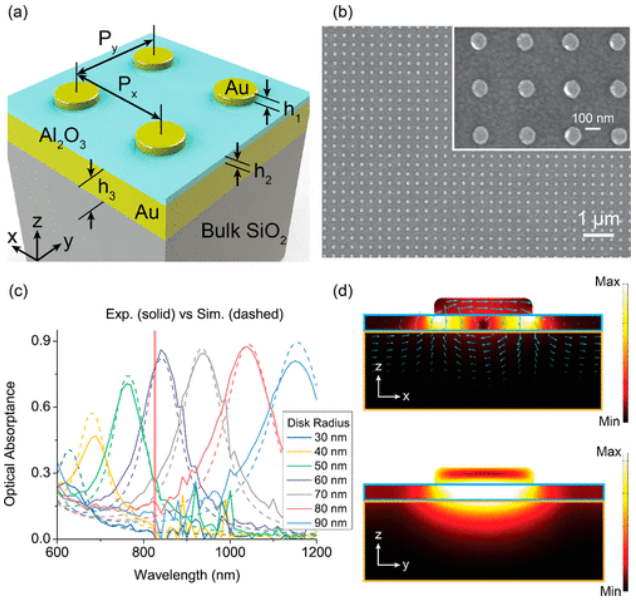

Figure 13. (a) Schematic of the gap plasmon structure: the gold (Au) nanodisk array (NDA). (b) Scanning electron micrograph (SEM) of the fabricated NDA on Al2O3 and Au layers. Scale bar: 1 μm. Inset: zoomed-in view of the NDA showing a few nanodisks. Scale bar: 100 nm. The nanodisks in both images have a designated radius of 60 nm. (c) Measured (solid lines) and simulated (dashed lines) optical absorptance spectra of the NDAs with disk radii ranging from 30 to 90 nm. (d) Simulated electric (upper panel) and magnetic (lower panel) field amplitudes at two orthogonal planes when the NDA is under resonant excitation (60 nm radius nanodisk under 840 nm incident light). The incident light is linearly polarized along the x direction.

References

[1] N. Kinsey, M. Ferrera, V. M. Shalaev, and A. Boltasseva, "Examining nanophotonics for integrated hybrid systems: a review of plasmonic interconnects and modulators using traditional and alternative materials [Invited]," *J. Opt. Soc. Am. B*, vol. 32, no. 1, p. 121, Jan. 2015.

[2] B. You, J.-Y. Lu, T.-A. Liu, and J.-L. Peng, "Hybrid terahertz plasmonic waveguide for sensing applications," *Opt. Express*, vol. 21, no. 18, p. 21087, Sep. 2013.

[3] M. L. Brongersma, N. J. Halas, and P. Nordlander, "Plasmon-induced hot carrier science and technology," *Nat. Nanotechnol.*, vol. 10, no. 1, pp. 25–34, Jan. 2015.

[4] V. J. Sorger, N. D. Lanzillotti-Kimura, R.-M. Ma, and X. Zhang, "Ultra-compact silicon nanophotonic modulator with broadband response," *Nanophotonics*, vol. 1, no. 1, pp. 17–22, Jan. 2012.

[5] A. Boltasseva, T. Nikolajsen, K. Leosson, K. Kjaer, M. S. Larsen, and S. I. Bozhevolnyi, "Integrated optical components utilizing long-range surface plasmon polaritons," *J. Light. Technol.*, vol. 23, no. 1, pp. 413–422, Jan. 2005.

[6] N. R. Fong, P. Berini, and R. N. Tait, "Hydrogen sensing with Pd-coated long-range surface plasmon membrane waveguides," *Nanoscale*, vol. 8, no. 7, pp. 4284–4290, 2016.

[7] N. Kinsey, M. Ferrera, G. V. Naik, V. E. Babicheva, V. M. Shalaev, and A. Boltasseva, "Experimental demonstration of titanium nitride plasmonic interconnects," *Opt. Express*, vol. 22, no. 10, p. 12238, May 2014.

[8] A. S. Roberts, A. Pors, O. Albrektsen, and S. I. Bozhevolnyi, "Subwavelength plasmonic color printing protected for ambient use," *Nano Lett.*, 2014.

[9] A. Manjavacas, J. G. Liu, V. Kulkarni, and P. Nordlander, "Plasmon-Induced Hot Carriers in Metallic Nanoparticles," *ACS Nano*, vol. 8, no. 8, pp. 7630–7638, Aug. 2014.

[10] N. Kinsey, C. DeVault, J. Kim, M. Ferrera, V. M. Shalaev, and A. A. Boltasseva, "Epsilon-near-zero Al-doped ZnO for ultrafast switching at telecom wavelengths," *Optica*, vol. 2, no. 7, pp. 616–622, Jul. 2015.

Appendix

Archival Publications supported in full or in part by this grant

(1) Haffner, C.; Chelladurai, D.; Fedoryshyn, Y.; Josten, A.; Baeuerle, B.; Heni, W.; Watanabe, T.; Cui, T.; Cheng, B.; Saha, S.; Elder, D. L.; Dalton, L. R.; Boltasseva, A.; Shalaev, V. M.; Kinsey, N.; Leuthold, J. Low-Loss Plasmon-Assisted Electro-Optic Modulator. Nature 2018, 556 (7702), 483–486. https://doi.org/10.1038/s41586-018-0031-4.

(2) Saha, S.; Dutta, A.; Kinsey, N.; Kildishev, A. V.; Shalaev, V. M.; Boltasseva, A. On-Chip Hybrid Photonic-Plasmonic Waveguides with Ultrathin Titanium Nitride Films. ACS Photonics 2018, 5 (11), 4423–4431. https://doi.org/10.1021/acsphotonics.8b00885.

(3) Dutta, A.; Naldoni, A.; Malara, F.; Govorov, A. O.; Shalaev, V. M.; Boltasseva, A. Gap-Plasmon Enhanced Water Splitting with Ultrathin Hematite Films: The Role of Plasmonic-Based Light Trapping and Hot Electrons. In Faraday Discussions; Royal Society of Chemistry, 2019; Vol. 214, pp 283–295. https://doi.org/10.1039/c8fd00148k.

(4) Mascaretti, L.; Dutta, A.; Kment, Š.; Shalaev, V. M.; Boltasseva, A.; Zbořil, R.; Naldoni, A. Plasmon-Enhanced Photoelectrochemical Water Splitting for Efficient Renewable Energy Storage. Adv. Mater. 2019, 31 (31), 1805513. https://doi.org/10.1002/adma.201805513.

(5) Song, M.; Wang, D.; Peana, S.; Choudhury, S.; Nyga, P.; Kudyshev, Z. A.; Yu, H.; Boltasseva, A.; Shalaev, V. M.; Kildishev, A. V. Colors with Plasmonic Nanostructures: A Full-Spectrum Review. Applied Physics Reviews. American Institute of Physics Inc. October 25, 2019, p 41308. https://doi.org/10.1063/1.5110051.

(6) Nyga, P.; Chowdhury, S. N.; Kudyshev, Z.; Thoreson, M. D.; Kildishev, A. V; Shalaev, V. M.; Boltasseva, A. Laser-Induced Color Printing on Semicontinuous Silver Films: Red, Green and Blue. Opt. Mater. Express 2019, 9 (3), 1528. https://doi.org/10.1364/ome.9.001528.

(7) Xu, X.; Dutta, A.; Khurgin, J.; Wei, A.; Shalaev, V. M.; Boltasseva, A. TiN@TiO 2 Core–Shell Nanoparticles as Plasmon-Enhanced Photosensitizers: The Role of Hot Electron Injection. Laser Photon. Rev. 2020, 14 (5), 1900376. https://doi.org/10.1002/lpor.201900376.

(8) George, H.; Reed, J.; Ferdinandus, M.; DeVault, C.; Lagutchev, A.; Urbas, A.; Norris, T. B.; Shalaev, V. M.; Boltasseva, A.; Kinsey, N. Nonlinearities and Carrier Dynamics in Refractory Plasmonic TiN Thin Films. Opt. Mater. Express 2019, 9 (10), 3911. https://doi.org/10.1364/OME.9.003911.

(9) Diroll, B. T.; Saha, S.; Shalaev, V. M.; Boltasseva, A.; Schaller, R. D. Broadband Ultrafast Dynamics of Refractory Metals: TiN and ZrN. (In print. Advanced Optical Materials) 2020, 1–39.

(10) Reddy, H.; Wang, K.; Kudyshev, Z.; Zhu, L.; Yan, S.; Vezzoli, A.; Higgins, S. J.; Gavini, V.; Boltasseva, A.; Reddy, P.; Shalaev, V. M.; Meyhofer, E. Determining Plasmonic Hot-Carrier Energy

Distributions via Single-Molecule Transport Measurements. Science (80-.). 2020, eabb3457. https://doi.org/10.1126/science.abb3457.

(11) Kudyshev, Z. A.; Kildishev, A. V.; Shalaev, V. M.; Boltasseva, A. Machine-Learning-Assisted Metasurface Design for High-Efficiency Thermal Emitter Optimization. Appl. Phys. Rev. 2020, 7 (2), 021407. https://doi.org/10.1063/1.5134792.

(12) Naldoni, A.; Kudyshev, Z. A.; Mascaretti, L.; Sarmah, S. P.; Rej, S.; Froning, J. P.; Tomanec, O.; Yoo, J. E.; Wang, D.; Kment, Š.; Montini, T.; Fornasiero, P.; Shalaev, V. M.; Schmuki, P.; Boltasseva, A.; Zbořil, R. Solar Thermoplasmonic Nanofurnace for High-Temperature Heterogeneous Catalysis. Nano Lett. 2020, 20 (5), 3663–3672. https://doi.org/10.1021/acs.nanolett.0c00594.

Selected conference proceedings supported by the grant:

(1) A. Boltasseva, H. V. Reddy, U. Guler, Z.A. Kudyshev, S.I. Azzam, K. Chaudhuri, A. V. Kildishev, and V.M. Shalaev, in *Plasmon. Des. Mater. Fabr. Charact. Appl. XVII*, edited by T. Tanaka and D.P. Tsai (SPIE, 2019), p. 26.

(2) D. Shah, K. Chaudhuri, Z. Wang, A. Catellani, M. Alhabeb, H. Reddy, X. Meng, S. Azzam, N. Kinsey, A. Kildishev, Y. Kim, V. Shalaev, A. Calzolari, Y. Gogotsi, and A. Boltasseva, in *Smart Photonic Optoelectron. Integr. Circuits XXI*, edited by E.-H. Lee and S. He (SPIE, 2019), p. 34.

(3) Z. Kudyshev, A. Boltasseva, A. V. Kildishev, and V.M. Shalaev, in *Photonic Phononic Prop. Eng. Nanostructures IX*, edited by A. Adibi, S.-Y. Lin, and A. Scherer (SPIE, 2019), p. 54.

(4) Z.A. Kudyshev, S. Bogdanov, A. V. Kildishev, A. Boltasseva, and V.M. Shalaev, in *Metamaterials, Metadevices, Metasystems 2019*, edited by N. Engheta, M.A. Noginov, and N.I. Zheludev (SPIE, 2019), p. 90.

(5) A. Boltasseva, C. DeVault, V. Bruno, S. Saha, Z. Kudyshev, A. Dutta, S. Vezzoli, M. Ferrera, D. Faccio, and V.M. Shalaev, in *Oxide-Based Mater. Devices X*, edited by F.H. Teherani, D.C. Look, and D.J. Rogers (SPIE, 2019), p. 58.

(6) A. Boltasseva, in *Metamaterials, Metadevices, Metasystems 2019*, edited by N. Engheta, M.A. Noginov, and N.I. Zheludev (SPIE, 2019), p. 47.

(7) A. Dutta, A. Naldoni, A. Govorov, V. M. Shalaev, A. Boltasseva, in *2019 Conf. Lasers Electro-Optics, CLEO 2019 - Proc.*, **2019**.[8] A. Boltasseva, H. V. Reddy, U. Guler, Z. A. Kudyshev, S. I. Azzam, K. Chaudhuri, A. V. Kildishev, V. M. Shalaev, in *Plasmon. Des. Mater. Fabr. Charact. Appl. XVII* (Eds.: T. Tanaka, D.P. Tsai), SPIE, **2019**, p. 26.

List of Patents filed in the Project Period:

[1] Laser-induced Color Printing on Nanostructured Plasmonic Films, patent application, 2020